



Nonlinear Analysis: Modelling and Control
ISSN: 1392-5113
ISSN: 2335-8963
nonlinear@mii.vu.lt
Vilniaus Universitetas
Lituania

Modeling the recent outbreak of COVID-19 in India and its control strategies

Kumar Upadhyay, Ranjit; Acharya, Sattwika

Modeling the recent outbreak of COVID-19 in India and its control strategies


Nonlinear Analysis: Modelling and Control, vol. 27, núm. 2, 2022

Vilniaus Universitetas, Lituania

Disponible en: <https://www.redalyc.org/articulo.oa?id=694173128004>

DOI: <https://doi.org/10.15388/namc.2022.27.25197>

Modeling the recent outbreak of COVID-19 in India and its control strategies

Ranjit Kumar Upadhyay ranjitupadhyay@iitism.ac.in
Indian Institute of Technology (Indian School of Mines), India
 <https://orcid.org/0000-0002-1210-7804>
 Sattwika Acharya sattwikacharya@gmail.com
Indian Institute of Technology (Indian School of Mines), India

Nonlinear Analysis: Modelling and Control, vol. 27, núm. 2, 2022

Vilniaus Universitetas, Lituania

Recepción: 29 Enero 2021
 Revisado: 19 Agosto 2021
 Publicación: 06 Enero 2022

DOI: <https://doi.org/10.15388/namc.2022.27.25197>

Redalyc: <https://www.redalyc.org/articulo.oa?id=694173128004>

Abstract: The recent emergence of COVID-19 has drawn attention to the various methods of disease control. Since no proper treatment is available till date and the vaccination is restricted to certain age groups, also vaccine efficacy is still under progress, the emphasis has been given to the method of isolation and quarantine. This control is induced by tracing the contacts of the infectious individuals, putting them to the quarantine class and based on their symptoms, classifying them either as the susceptible or sick individuals and moving the sick individuals to the isolated class. To track the current pandemic situation of COVID-19 in India, we consider an extended Susceptible-Exposed-Quarantine-Infected-Isolated-Recovered (SEQ₁ IQ₂ R) compartmental model along with calculating its control reproductive number R_c . The disease can be kept in control if the value of R_c remains below one. This “threshold” value of R_c is used to optimize the period of quarantine, and isolation and have been calculated in order to eradicate the disease. The sensitivity analysis of R_c with respect to the quarantine and isolation period has also been done. Partial rank correlation coefficient method is applied to identify the most significant parameters involved in R_c . Based on the observed data, 7-days moving average curves are plotted for prelockdown, lockdown and unlock 1 phases. Following the trend of the curves for the infection, a generalized exponential function is used to estimate the data, and corresponding 95% confidence intervals are simulated to estimate the parameters. The effect of control measures such as quarantine and isolation are discussed. Following various mathematical and statistical tools, we systematically explore the impact of lockdown strategy in order to control the recent outbreak of COVID-19 transmission in India.

Keywords: COVID-19, lockdown, controlled reproduction number, sensitivity analysis, confidence interval.

1 Introduction

In recent studies on COVID-19, it has been noticed that nearly all individuals included had symptoms since the presence of symptoms was used to determine whether someone would be admitted for a test of COVID-19 or not. However, it is possible that some individuals may be infected and be able to transmit to others without developing symptoms. Recent studies show that asymptomatic individuals were also screened for infection and tested positive. The study also suggests the possibility of presymptomatic transmission. In general, compartmental epidemiological models assume that the onset of symptoms and the onset

of infectiousness coincide, but recent evidence indicates that symptoms may be delayed relative to when an individual is infectious. Viral loads are measured over time in symptomatic individuals, studies show that they are at a peak on the first day of symptoms, suggesting that they were already high before symptoms started [23]. COVID-19, the recent emergence of the early spread of severe acute respiratory syndrome coronavirus 2 (SARS-CoV-2) has been announced as a pandemic by the World Health Organization (WHO) on March 11, 2020. It was first identified in December 2019 in Wuhan, the capital of Hubei, China, and now is an increasing concern about COVID-19 worldwide. It belongs to the Coronaviridae family in the Nidovirales order [16]. It is a RNA virus and has symptoms, which are very much similar to normal influenza virus. Also it takes around 3 to 4 days to show the symptoms [15]. It can be transmitted by three main routes including direct transmission, contact transmission and aerosol [17]. According to an estimate by WHO, in early stages, the disease is less contagious than smallpox, chickenpox and mumps, but more contagious than similar kinds of disease like seasonal flu and MERS. The estimated disease fatality rate for COVID-19 is 3.4%, which is less than that of smallpox, SARS and MERS [8]. As of now, almost every country has been affected by this pandemic with 90.3 millions total cases across the world with more than 19,33,487 deaths. The first appearance of Human coronaviruses was identified in the mid-1960s. Since then, considerable outbreaks caused by other variants of corona virus, namely, SARS in 2003 in mainland China, MERS in 2012 in Saudi Arabia, MERS outbreak in 2015 in South Korea. As a result, SARS-CoV (2003) infected 8098 individuals with mortality rate of 9% across 26 countries in the world, and MERS-coronavirus infected more than 2428 individuals and 838 deaths [16]. On the other hand, novel corona virus (2019) infected 90.3 million individuals with around 1.935 million deaths across 218 countries till date of this writing. After the outbreak of COVID-19 in Wuhan, the infection spread rapidly to all provinces and cities in China. During the early stages, this spread was due to insufficient understanding of the transmission mechanism of the virus, as well as increases in population mobility during the Spring festival. However, after the lockdown of Wuhan on 23 January 2020 and the strengthening of prevention and control measures in various regions, the epidemic situation in all provinces and autonomous regions was effectively contained, and the epidemic situation improved within a short period.

In India, the first case of COVID-19 was reported on January 30, 2020 in Thrissur district of Kerala. It was an imported case. The patient was a student of Wuhan University, China. Initially, a gradual increase was observed in the spreading of the disease, but it took about three months to reach a lethal state. Acknowledging the severity of the situation, the Indian Government announced a 21-day country-wide lockdown as a preventive measure for the COVID-19 outbreak on 24th March, 2020. To study the outbreak and transmission dynamics in India, Sardar et al. [14] considered a new mathematical model on COVID-19 with and

without lockdown effect. By validating the model to the data on notified cases from five different states and overall India, authors estimated several epidemiologically important parameters including ... In the second week of January 2021, India recorded 1.51 lakh deaths due to COVID-19 pandemic, accounting for 7.8% of the global tally of 19.35 lakh. Its cumulative fatality rate (CFR) of 1.4% is lower than the global average of 2.2% [26].

From the perspective of understanding the dynamics of the pandemic, several disease modeling approaches have been tried. Compartmental models are the simplest way out to study an epidemic. As the dynamics of the disease depends upon contact between people, an age-structured model can be helpful in providing key insights, which can be instrumental in developing policies to control the outbreak [21]. This kind of model can be used to study the effect of physical distancing measures ranging from staying at home, leaving home for essential services, closure of schools and colleges and the reopening of nonessential sectors. Some authors tried to show the closure effects in terms of resetting the susceptible people with good old SIR model, but this oversimplification does not allow to understand measures taken in different fields like school, work or other activities [2]. Delay differential equations had been also used in predicting future condition along with examination of health care capacity in the pandemic in vaccine-free scenario [1]. Recently, Rohith and Devika [12] proposed an SEIR model with nonlinear incidence rates and studied the dynamics and control of COVID-19 pandemic. In order to verify its efficacy, the control strategies are then compared with real-time data. Besides this, attention has been drawn to the strategies of isolation and quarantine as a method of disease control [7]. The controlled reproduction number R_c is another component, which is of great significance since it represents the value of the basic reproduction number in presence of control measures. The disease will be eliminated if $R_c < 1$ and when $R_c > 1$, it means that each individual affected by a transmittable disease is expected to infect exponentially, and the disease is expected to spread through the susceptible population. On the other hand, the disease gets fade away of the population when $R_c < 1$ and thus the disease transmission can be regulated to either one or less than that for each case [22]. Tian et al. [20] presented a study on the effects of control strategies on COVID-19 transmission in Wuhan during the first 50 days from December 31, 2019 to February 19, 2020. They claimed that lockdown measure makes the people outside Wuhan to cope with the COVID-19 ahead of time. In this paper, we proposed a new compartment model to track the current pandemic situation in India, calculated the controlled reproduction number R_c , perform the sensitivity analysis of R_c with respect to quarantine and isolation period. To identify the role of the significant parameters, PRCC test has been applied.

The paper is organized as follows: In Section 2, a new mathematical model is constructed, including the effect of quarantine and isolation. Section 3 deals with the positivity and boundedness of the solution. Also

disease-free equilibrium and control reproduction number are calculated. Sensitivity analysis of control reproduction number R_c with respect to the control parameters ρ and σ have been carried out in Section 4. We have used partial rank correlation coefficient (PRCC) method to describe the relationship among R_c and other parameters. The estimation of epidemiological parameters is done in Section 5, corresponding to the various classified time span including initial prelockdown phase, lockdown phases and the unlock 1 phase together with the effect of quarantine and isolation in the model, and the main contribution of this work is concluded in Section 6.

2 Formulation of the mathematical model

We have designed a compartmental model following the approach considered in Martcheva [11]. We split the total population of size N into individuals, who are susceptible to the disease S ; exposed individuals E ; quarantined individuals Q_1 ; infective nonisolated individuals I ; isolated individuals Q_2 ; and recovered and immune individuals R . We assume that immunity is permanent. We denote the active population, that is, nonquarantined and nonisolated individuals, by $A = N - Q$, ($Q = Q_1 + Q_2$). Assuming that sick individuals and the traced individuals, who had either a journey history or were in contact with the infected individuals, stay at home and undergo some kind of isolation and quarantine, that reduces their ability to infect others. For simplicity, we assume that they do not infect anybody [11]. We further assume that the disease is basically fatal, especially, with the presence of comorbidity (a realistic assumption for COVID-19). The step by step model formulation can be described as follows:

Susceptible population $s(t)$. The class of healthy individuals, who are capable of contracting the disease, are called susceptible individuals. Here in this case, a constant recruitment of individuals is occurring at a rate Λ . Susceptible individuals S come into contact with infectious I at a rate β and exposed individuals E at a rate βq , and that move to the exposed class E . Traced susceptible individuals move to the quarantine class Q_1 at a rate ρ . Susceptible are reduced by a natural mortality rate μ . Quarantined individuals, those who show no symptoms, return to the susceptible class at a rate η_1 at the end of the quarantine. Thus, the rate of change of the size of S is determined by the following equation:

$$\frac{dS}{dt} = \Lambda - \beta \frac{S(I + qE)}{N - Q} - \rho S - \mu S + \eta_1 Q_1.$$

Exposed population $E(t)$. In the transmission dynamics of the exposed populations, a continuous flow of susceptible individuals S , who come into a contact with infectious I at a rate β and exposed individuals E at a rate βq . Traced exposed individuals move to the quarantine class

at a rate ρ . At the end of the quarantine period, a number of exposed individuals, who are not traced move to the infected class at a rate γ . Exposed individuals have the natural mortality rate μ . Thus, the governing equation is

$$\frac{dE}{dt} = \beta \frac{S(I + qE)}{N - Q} - (\rho + \mu + \gamma)E.$$

Quarantine population $Q_1(t)$. In order to prevent the spread of a disease, the traced individuals coming in contact with the infectious one are taken separately, these individuals are called quarantined. ρ denotes the rate of movement of the exposed individuals to the quarantine class. Quarantined individuals Q_1 , those who have no symptoms return to the susceptible class at a rate η_1 . After the end of the quarantine state, the sick individuals are move to the isolated class Q_2 at a rate η_2 . The natural mortality rate for the quarantined is μ . The resulting equation become

$$\frac{dQ_1}{dt} = \rho S + \rho E - (\mu + \eta_1 + \eta_2)Q_1.$$

Infected population $I(t)$. The individuals, who can become the cause of an infection and are able to transmit the disease, are called infectious. An inflow of infected exposed individual at a rate γ . The infected, who are tested positive of COVID-19, are isolated at a rate σ . COVID-19 is a fatal disease in some cases, d denotes the disease related death rate. μ denotes the natural death rate. Therefore, the corresponding equation is

$$\frac{dI}{dt} = \gamma E - (\mu + \sigma + d)I.$$

Isolated population $Q_2(t)$. In case of a contagious disease, the process of isolation is used to separate the infectious one from the healthy susceptible individual. Usually, the hospitals are places to keep those isolated individuals in order to reduce the spread of the disease. In our model, the isolated individuals are kept isolated at a rate σ . After the quarantine stage, those who have showed symptoms and tested positive of COVID-19, are kept to the isolated compartment at a rate η_2 . Some of the isolated individuals are getting recovered at a rate η_3 . Isolated individuals have natural mortality rate μ . The rate of change of isolated individual is given as

$$\frac{dQ_2}{dt} = \sigma I + \eta_2 Q_1 - (r + \mu) Q_2.$$

Recovered population $R(t)$. The class of individuals, who recovers and return to the healthy susceptible class, are called removed/recovered individuals R . In this case the recovered individuals are moving in this compartment with a rate r . Natural death rate for the recovered individuals is μ . Therefore, the recovered compartment is changing with time as

$$\frac{dR}{dt} = rQ_2 - \mu R.$$

The above assumptions result in the following system of ordinary differential equation:

$$\begin{aligned} \frac{dS}{dt} &= \Lambda - \beta \frac{S(I + qE)}{N - Q} - (\mu + \rho)S + \eta_1 Q_1, \\ \frac{dE}{dt} &= \beta \frac{S(I + qE)}{N - Q} - (\mu + \rho + \gamma)E, \\ \frac{dQ_1}{dt} &= \rho S + \rho E - (\mu + \eta_1 + \eta_2)Q_1, \\ \frac{dQ_2}{dt} &= \sigma I + \eta_2 Q_1 - (\mu + r)Q_2, \\ \frac{dI}{dt} &= \gamma E - (\mu + \sigma + d)I, \quad \frac{dR}{dt} = rQ_2 - \mu R \end{aligned} \tag{1}$$

with initial condition $S(0) > 0, E(0) > 0, Q_1(0) > 0, I(0) > 0, Q_2(0) > 0, R(0) > 0$. The biological meaning of all the parameters and their numerical values are given in Table 1 (p. 10) and are taken from [11] and other literature.

3 Mathematical analysis

3.1 Positivity and boundedness of the solution

In this section, we provide the proof for the positivity and boundedness of solutions of system (1) with initial conditions $(S(0), E(0), Q_1(0), I(0), Q_2(0), R(0)) \in \mathbb{R}_+^6$. We state the following propositions.

Proposition 1. *System (1) is invariant in \mathbb{R}_+^6 .*

Proof. By rewriting system (1) as

$$\frac{dX}{dt} = M(X(t)), \quad X(0) = X_0 \geq 0,$$

$X = (S, E, Q_1, I, Q_2, R)^T$, $M(X(t)) = (M_1(X), M_2(X), \dots, M_6(X))^T$, we note that

$$\begin{aligned} \left. \frac{dS}{dt} \right|_{S=0} &= \Lambda + \eta_1 Q_1 \geq 0, & \left. \frac{dE}{dt} \right|_{E=0} &= \beta \frac{SI}{N-Q} \geq 0, \\ \left. \frac{dQ_1}{dt} \right|_{Q_1=0} &= \rho S + \rho E \geq 0, & \left. \frac{dQ_2}{dt} \right|_{Q_2=0} &= \sigma I + \eta_2 Q_1 \geq 0, \\ \left. \frac{dI}{dt} \right|_{I=0} &= \gamma E \geq 0, & \left. \frac{dR}{dt} \right|_{R=0} &= r Q_2 \geq 0. \end{aligned}$$

The above is true for any point belonging to the interior of \mathbb{R}_+^6 or on the boundary of the hyperplanes. It implies that system (1) is invariant in \mathbb{R}_+^6 .

Proposition 2. *System (1) is bounded in the region*

$$\Omega = \left\{ (S, E, Q_1, I, Q_2, R) \in \mathbb{R}_+^6 : S + E + Q_1 + I + Q_2 + R \leq \frac{\Lambda}{\mu} \right\}.$$

Proof. The overall population $N = S + E + Q_1 + I + Q_2 + R$ obeys

$$\begin{aligned} \frac{dN}{dt} &= \frac{dS}{dt} + \frac{dE}{dt} + \frac{dQ_1}{dt} + \frac{dI}{dt} + \frac{dQ_2}{dt} + \frac{dR}{dt} \\ &= \Lambda - \mu N - dI. \end{aligned}$$

In absence of the disease (initially, when $I = 0$),

$$\frac{dN}{dt} = \Lambda - \mu N.$$

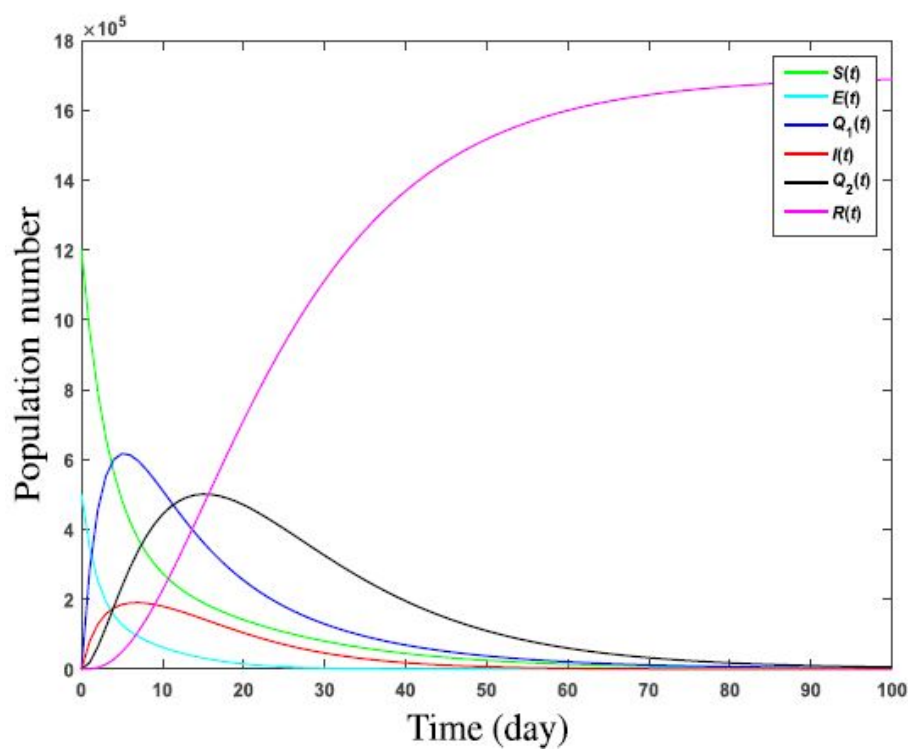


Figure 1.
The time series of the population in system (1).

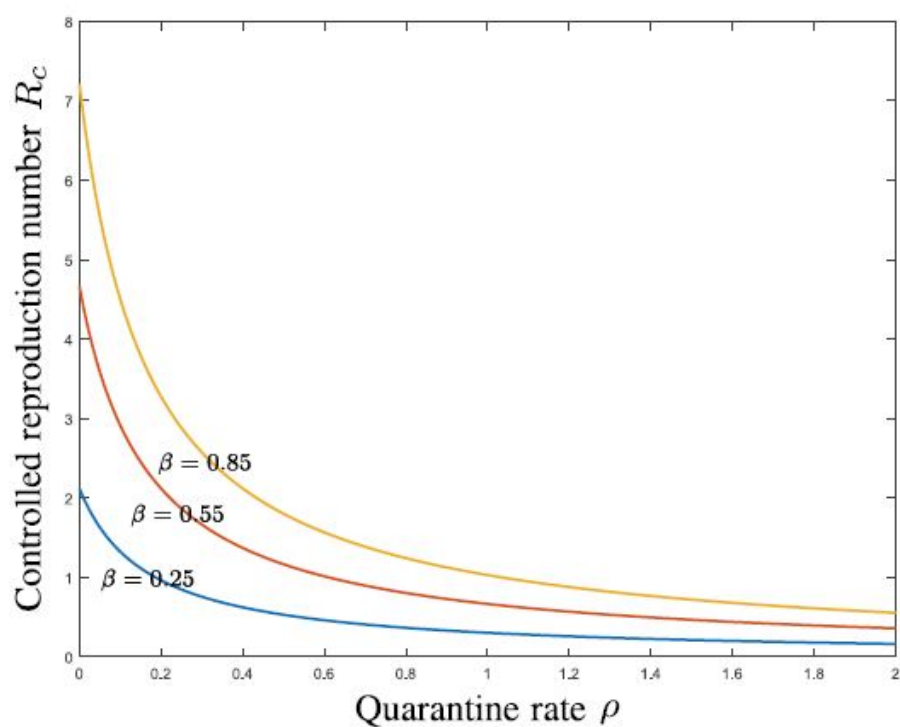


Figure 2.
The controlled reproduction number as a decreasing function of ρ for different values of β .

This shows that the population size N tends to its carrying capacity Λ/μ as $t \rightarrow \infty$, implying that the solution of (1) exists in the region defined by

$$\Omega = \left\{ (S, E, Q_1, I, Q_2, R) \in \mathbb{R}_6^+ : S + E + Q_1 + I + Q_2 + R \leq \frac{\Lambda}{\mu} \right\}.$$

Figure 1 shows that initially the number of susceptible is high enough, but finally it approaches asymptotically towards zero, while recovered individuals are gradually rising with time. Besides this, the number of infected, quarantined and isolated individuals show a growth in the beginning and eventually reduces the slopes of the curves as time progresses. Exposed population exhibits a downturn towards the end of the time scale. These time series behavior is supporting the real world phenomena. Figure 2 is plotted to show the inverse relationship between the controlled reproduction number R_c and the quarantine rate ρ with various values of transmission rate β . Here it is clear that as the value of β is getting larger, the slope of the curve is declining faster.

3.2 Disease-free equilibrium and control reproduction number

Looking for the equilibria of system (1), we discover that there is always a disease-free equilibrium $E^0(S^0, E^0, Q_1^0, I^0, Q_2^0, R^0)$, where, $S^0 = \Lambda/\mu, E^0 = Q_1^0 = I^0 = Q_2^0 = R^0 = 0$. The controlled reproduction number is the value of the basic reproduction number in presence of control measures (quarantine and isolation) [5]. It is a dimensionless quantity and is denoted by R_c . We can calculate this quantity by using the next-generation operator method [4, 6]. For this, we construct the compartments, which are infected from system (1) and decompose the right-hand side as

$$\frac{dX}{dt} = \mathcal{F} - \mathcal{V},$$

where F and V respectively represents the rate of appearance of new infections and the transitional terms such as recruitment, deaths, disease transmission and recovery. In this case,

$$\mathcal{F} = \begin{pmatrix} \frac{\beta S(I+qE)}{S+E+I+R} \\ 0 \\ 0 \\ 0 \end{pmatrix}, \quad \mathcal{V} = \begin{pmatrix} (\rho + \mu + \gamma)E \\ -\rho S - \rho E + (\mu + \eta_1 + \eta_2)Q_1 \\ -\gamma E + (\mu + \sigma + d)I \\ -\sigma I - \eta_2 Q_1 + (\mu + r)Q_2 \end{pmatrix}$$

Now we calculate the Jacobian of F and V at DFE, E_0 as

$$F = \frac{\partial \mathcal{F}}{\partial X} = \begin{pmatrix} \frac{q\beta S(S+I+R)}{(S+E+I+R)^2} & 0 & \frac{\beta S(S+E+R)}{(S+E+I+R)^2} & 0 \\ 0 & 0 & 0 & 0 \\ 0 & 0 & 0 & 0 \\ 0 & 0 & 0 & 0 \end{pmatrix}$$

And

$$V = \frac{\partial \mathcal{V}}{\partial X} = \begin{pmatrix} \rho + \mu + \gamma & 0 & 0 & 0 \\ -\rho & \mu + \eta_1 + \eta_2 & 0 & 0 \\ -\gamma & 0 & \mu + \sigma + d & 0 \\ 0 & \eta_2 & -\sigma & \mu + r \end{pmatrix},$$

$$J_0 = \frac{\partial \mathcal{F}}{\partial X} = \begin{pmatrix} -(\mu + \rho) & -\beta q & \eta_1 & -\beta & 0 & 0 \\ 0 & \beta q - (\mu + \rho + \gamma) & 0 & \beta & 0 & 0 \\ \rho & \rho & -(\mu + \eta_1 + \eta_2) & 0 & 0 & 0 \\ 0 & \gamma & 0 & -(\mu + \sigma + d) & 0 & 0 \\ 0 & 0 & \eta_2 & \sigma & -(\mu + r) & 0 \\ 0 & 0 & 0 & 0 & r & -\mu \end{pmatrix}$$

Following Heffernan et al. [9], $R_c = \rho(FV^{-1})$, where ρ is the spectral radius of the next-generation matrix FV^{-1} . Thus, from model (1) we have the following expression for R_c :

$$R_c = \frac{\beta \gamma}{(\rho + \mu + \gamma)(\mu + \sigma + d)} + \frac{\beta q}{\rho + \mu + \gamma}.$$

Here, in absence of the control measures (isolation rate $\sigma = 0$ and quarantine rate $\rho = 0$), the basic reproduction number R_c can be written as

$$R_0 = \frac{\beta \gamma}{(\mu + \gamma)(\mu + d)} + \frac{\beta q}{\mu + \gamma}.$$

The first part of the controlled reproduction number indicates the number of secondary infections generated by the infectious individuals, and in the second part, it can be found the secondary infection generated by the exposed individuals; $\gamma/(\gamma + \rho + \mu)$ represents the part of the exposed individuals, which progresses to the infectious class. Clearly, the reproduction number is a decreasing function of the quarantined rate ρ and the isolation rate σ . The critical isolation rate $R_c = 1$ is given by $\sigma^* = \beta \gamma / (\rho + \mu + \gamma - \beta q) - (\mu + d)$.

The reproduction number, as a function of σ and ρ , is plotted in Fig. 3.

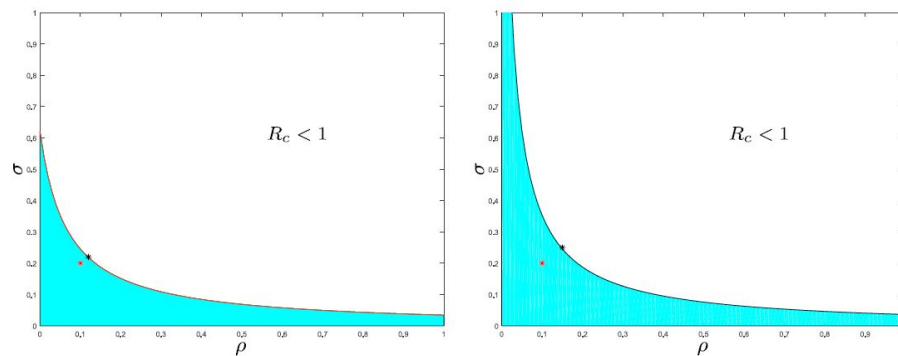


Figure 3.

Region representing $R_c > 1$, the pointed endemic situation with a red point, and the closest point on the curve $R_c = 1$ in black, corresponding to the values $q = 0.4$ and $q = 0.6$, respectively.

Theorem 1. *The disease-free equilibrium $E^0(A/\mu, 0, 0, 0, 0)$ is given by J_0 is locally asymptotically stable.*

Proof. The Jacobian matrix of system (1) around $E^0(A/\mu, 0, 0, 0, 0)$ is given by J_0 . Clearly, $-\mu$ and $-(\mu + r)$ are the two eigenvalues of J_0 . The other four eigenvalues are obtained from the submatrix

$$J_1 = \begin{pmatrix} -(\mu + \rho) & -\beta q & \eta_1 & -\beta \\ 0 & \beta q - T & 0 & \beta \\ \rho & \rho & -(\mu + \eta_1 + \eta_2) & 0 \\ 0 & \gamma & 0 & -(\mu + \sigma + d) \end{pmatrix},$$

where $T = \mu + \rho + \gamma$. These eigenvalues are the roots of the characteristic equation

$$\lambda^4 + A_1\lambda^3 + A_2\lambda^2 + A_3\lambda + A_4 = 0,$$

where

$$\begin{aligned} A_1 &= 4\mu + 2\rho + \gamma + \eta_1 + \eta_2 + \sigma + d - \beta q, \\ A_2 &= (\mu + \rho)(\mu + \rho + \gamma - \beta q) + (\mu + \eta_1 + \eta_2)(\mu + \sigma + d) \\ &\quad + (2\mu + 2\rho + \gamma - \beta q)(2\mu + \eta_1 + \eta_2 + \sigma + d) - \beta\gamma - \eta_1\rho, \\ A_3 &= (\mu + \rho)(\mu + \rho + \gamma - \beta q) + (\mu + \eta_1 + \eta_2)(\mu + \sigma + d) \\ &\quad \times (2\mu + 2\rho + \gamma - \beta q)(2\mu + \eta_1 + \eta_2 + \sigma + d) \\ &\quad - \beta\gamma(2\mu + \rho + \eta_1 + \eta_2) - \eta_1\rho(2\mu + \sigma + \rho + \gamma + d - \beta q), \\ A_4 &= (\mu + \rho)(\mu + \eta_1 + \eta_2)[(\mu + \rho + \gamma - \beta q)(\mu + \sigma + d) \\ &\quad - \beta\gamma] - \eta_1\rho[(\mu + \rho + \gamma - \beta q)(\mu + \sigma + d) - \beta\gamma] \\ &= ((\mu + \rho)(\mu + \eta_2) + \mu\eta_1)(\mu + \rho + \gamma)(\mu + \sigma + d)(1 - R_c). \end{aligned}$$

On solving, we have that other four eigenvalues of J_0 are obtained as
 There, all the eningevalues of J_0 are negative, and hence
 trace $J_0 < 0$ and $\det J_0 > 0$.

By Routh–Hurwitz criteria, we can conclude the local asymptotic stability of the disease- free equilibrium $E^0(A/\mu, 0, 0, 0, 0)$.

In Fig. 3, we have plotted the region $R_e > 1$ corresponding to two different values of $q = 0.4$ and $q = 0.6$. The region for $q = 0.6$ is larger and symmetric. The red point denotes the coordinates of the point provided in Table 2. The region $R_e > 1$ contains the point; hence, the corresponding rates of quarantine and isolation are same as given in Table 1. Therefore, the removal of the disease is not possible. Our aim will be to compute the required values of the rates of the quarantine and isolation obtained by small change to the values given in Table 1 for which the eradication of the disease is possible. To establish this, we try to find out the point on the curve representing $R_e = 1$ and the nearest to the red point. Following the approach given in [11], we consider (x, y) be the coordinates of the black point. The square of the distance between the two points is given by $(x - 0.1)^2 + (y - 0.2)^2$, where $(0.1, 0.2)$ is a coordinate of the red point. Furthermore, we replace ρ with x and σ with y in R_c . From the equation $R_e = 1$ we express σ as a function of p . The process of minimization leads us to differentiate the function with respect to x and equate the derivative to zero. This yields the equation

$$(x - 0.1) + (f(x) - 0.2)f'(x) = 0.$$

The corresponding coordinates of the black point is given as $(0.122, 0.227)$ and $(0.150, 0.2522)$ for the values of q as 0.4 and 0.6 , respectively. This gives us the idea how to modify the values of the rates of quarantine and isolation in order to eliminate the disease. If x denotes the coordinate of the black point, then the optimal new periods for quarantine and isolation can be given as $1/x$. These optimal periods that will cause expulsion are listed in Table 2. Table 2 suggests that changing the value of q from 0.4 to 0.6 , the contact tracing and quarantining has improved radically from 8 days to 6 days, while isolation should refine from 4 days to 3 days for the elimination of the disease.

Table 1.
Description of the parameters involved in model (1).

Parameter	Significance	Values (per day)
Λ	Recruitment rate of susceptible individuals	12, 00, 000
β	Transmission rate	0.25
ρ	Quarantine rate	0.21
μ	Natural death rate	0.00003914
d	Disease related death rate	0.001
γ	Rate of developing symptoms	0.2
σ	Isolation rate	0.1
η_1	Rate of coming back to susceptible class	0.1
η_2	Rate of development to infectiousness	0.1
r	Recovery rate for isolated individual	0.1
q	Reduction of infectivity of exposed individuals	0.18

Table 2.
Optimal periods for quarantine and isolation.

Strategy	$q = 0.4$	$q = 0.6$
$1/\rho$	8.187	6.660
$1/\sigma$	4.459	3.965

4 Sensitivity analysis of control reproduction number

4.1 Sensitivity and elasticity of the control parameters

Besides various control measures, it is important to describe the relative significance of the quarantine and isolation strategies with the controlled reproduction number R_c . We perform the sensitivity analysis of R_c as given in [3] to identify the significant parameters contributing variability in the outcome of the nondimensional quantity R_c for system (1). The sensitivity index of R_c with respect to the parameter ρ is

$$\zeta_{R_c}^{\rho} = \frac{\partial R_c}{\partial \rho} = -\frac{\beta\gamma}{(\rho + \mu + \gamma)^2(\mu + \sigma + d)} - \frac{\beta q}{(\rho + \mu + \gamma)^2}.$$

The elasticity index of quantity R_c with respect to the parameter ρ is given by

$$\varepsilon_{R_c}^{\rho} = -\frac{\rho}{\rho + \mu + \gamma}.$$

On putting the above values of the parameters, we have that $\varepsilon_{R_c}^{\rho} = -0.374945$ implies 10% increase in ρ and about 3.74945% decrease in R_c . Using mathematical and statistical techniques, the sensitivity analysis has been performed to regulate the significance of the epidemic model parameters. The sensitivity indices narrate us whether or not the infectious diseases will develop throughout the individuals. It is mainly utilized to describe the effectiveness of the reproduction number R_c to variation in the parameters of the system and also to point out the relative change in a state variable when a system parameter changes. The sensitivity index of R_c with respect to the parameter σ is defined as follows:

$$\zeta_{R_c}^{\sigma} = \frac{\partial R_c}{\partial \sigma} = -\frac{\beta\gamma}{(\rho + \mu + \gamma)(\mu + \sigma + d)^2}.$$

The elasticity index of quantity R_c with respect to the parameter σ is given by

$$\varepsilon_{R_c}^{\sigma} = -\frac{\sigma\gamma}{(\mu + \sigma + d)(\gamma + q(\sigma + \mu + d))}.$$

Numerical calculation gives that $\varepsilon_{R_c}^{\sigma} = -0.0362$ implies 10% increase in σ and will produce 0.3625% decrease in R_c . Besides this, it can be easily formulated that the sensitivity index of R_c with regards to the transmission rate R_c is free from any parameters. This represents that β is

$$\varepsilon_{R_c}^{\beta} = 1,$$

This represents that R_c the increasing function with respect to R_c . It implies that in the control and management of COVID-19, the probability of disease transmission is comparatively higher.

4.2 Global sensitivity analysis using partial rank correlation coefficient method

In this subsection, we will present the sensitivity analysis of the controlled reproduction number R to determine which parameters are important in contributing variability in the consequence of the nondimensional

quantity R_c for system (1). It is necessary to know the relative importance of the different parameters responsible for the transmission of COVID-19 in order to control and reduce human morbidity and mortality occurring due to corona virus [13]. Although the transmission of COVID-19 is directly related to the basic reproduction number R_0 in the beginning, but we have considered various control measures such as quarantine and isolation. We concentrate our studies regarding the controlled reproduction number R_c corresponding to system (1). The sensitivity indices of R_c show how crucial each parameter to the disease transmission. Here we use partial rank correlation coefficient (PRCC) method to find parameters that have a high impact on R_c and should be targeted by intervention strategies. It will be ideal to use both PRCC and extended Fourier amplitude sensitivity test (eFAST) to represent the relationship between the parameters, and output is not previously known. However, we discuss here only about the PRCC analysis.

The correlation coefficient measures the degree of linear relationship between two variables. It varies between -1 to +1. Partial correlation characterizes the same only while remaining inputs as discounted. Similarly, when the data are rank-transformed and a linear regression model is being described, it is called partial rank correlation (PRC). It measures the sensitivity for linear but monotonic relationships between the variables as long as little to no correlation exists between the inputs [10]. Thus, PRCC allows us to select which specific parameters should be considered for acquiring our goal. Since a priori information is not available, we assume the parameters as random variables with corresponding probability density function as of uniform distribution. Parameter values and ranges are adopted using the technique involved in Wu et al. [24]. The PRCC sensitivity results are carried out for R_c and are listed in Table 4 and also illustrated using bar charts in Fig. 4. The correlation value requires both a magnitude and a direction of either positive or negative. It is absolute and nondimensional value in the range from 1 to +1 without any units. As this value approaches closer to 1, the linear relationship becomes stronger between the two variables, regardless of the direction, and the zero correlation corresponds to no linear association among the variables. The calculated sensitivity indices of with the six different parameters involved in model (1) are shown in Table 4. The most significant parameters are the transmission rate β , the quarantine rate ρ and the isolation rate σ . Besides these, another influential parameter is the rate of developing symptoms γ as can be seen from Table 4 and bar charts in Fig. 4. The correlation coefficients that are ≤ 0.35 are generally considered to represent low or weak correlation [19]. In this case, the reduction of infectivity of exposed individuals q has correlation value as 0.2641, and also the natural mortality rate μ and disease related death rate d have significantly lower correlation. From Table 4 it can be observed that the parameters related to control measures (ρ and σ) have an inverse relationship whereas if the rate of quarantine and isolation increases, the value of controlled reproduction

number R_c decreases. Therefore, the sensitivity analysis suggest about the effectiveness of the control measures.

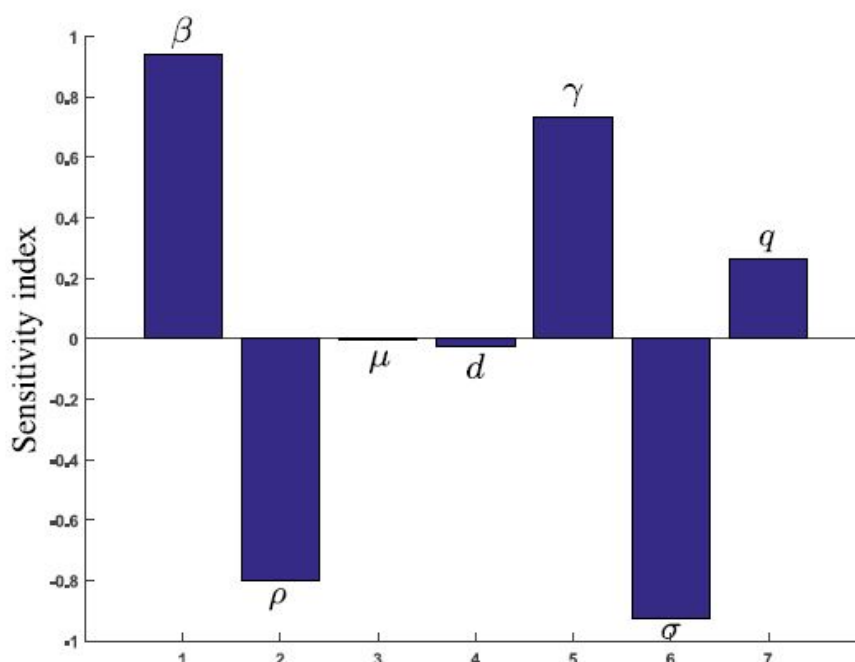


Figure 4.

Bar diagram showing the measure of sensitivity indices of R_c with the various parameters of model (1) and their reference values as mentioned in Table 4.

5 Estimation of epidemiological parameters

5.1 Data analysis

On March 22, 2020, the Indian government introduced the implementation of the nation- wide lockdown strategy in India to shut down the movement and to control the transmis- sion of COVID-19. Since March 01, 2020, based on the data provided by World Health Organization [25], we have analyzed the set of data reported for the confirmed cases of COVID-19 in India.

In order to get an overall idea about the set of data and while plotting those to avoid the peaks of the curve, we have considered here the 7- days moving average of the corre- sponding data set. The set of data are classified into the following groups:

- The initial prelockdown phase (March 01–21, 2020)
- Lockdown 1.0 (March 25–April 14, 2020)
- Lockdown 2.0 (April 15–May 03, 2020)
- Lockdown 3.0 (May 4–17, 2020)
- Lockdown 4.0 (May 18–31, 2020)
- Unlock 1.0 (June 1–30, 2020)

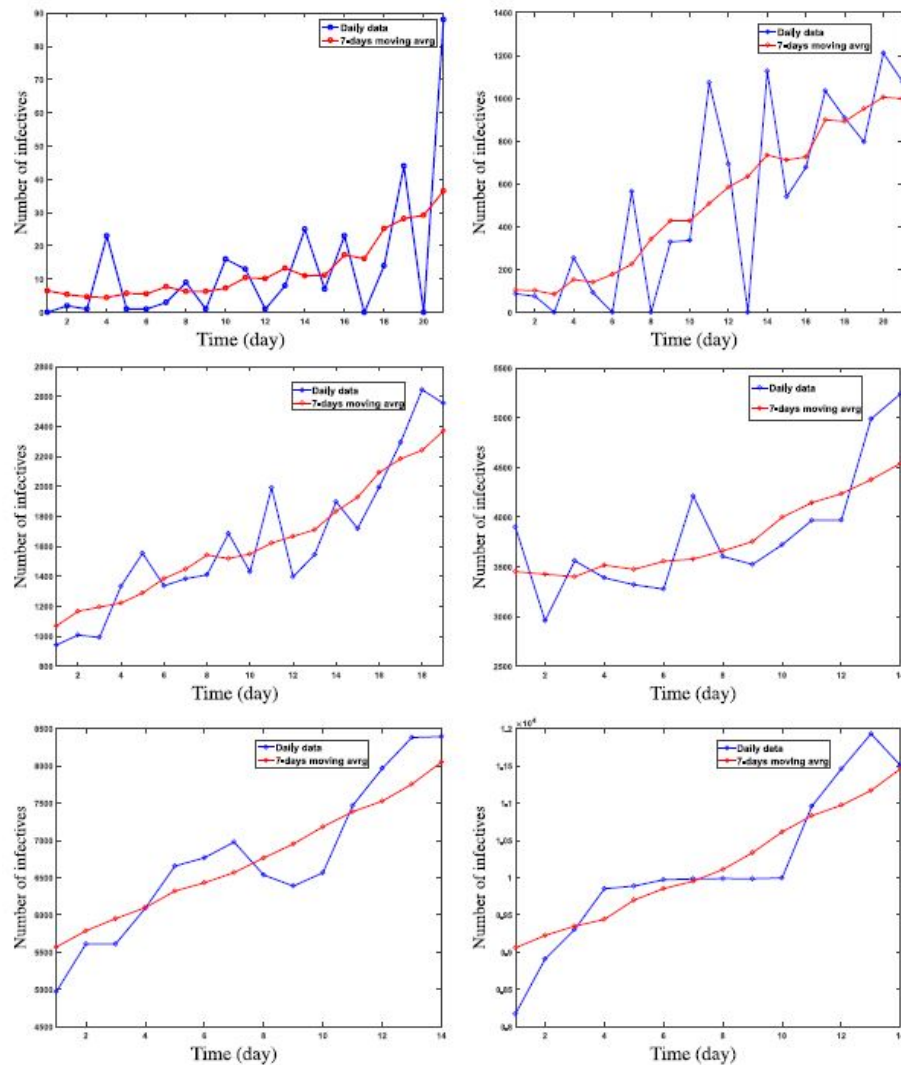


Figure 5.

7-days moving average of the infected cases in India for the six different group of data set.

During the lockdown phases, a strict community control strategy is applied to maintain the physical distancing since it become the only preventive measure in order to control the disease. This will lead to the control strategy by constructing the quarantine centers and keeping the infected individual isolated from the social contact/ movement. These are introduced in model (1), ρ and σ measure the rate of quarantine and isolation, respectively. Strict lockdown is the only way to control the community contact. In Fig. 5, the number of infected in each day is plotted along the y -axis, and the number of days are plotted in x -axis. In all the six figures, it has been shown that initially a gradual increase can be seen in the spread of the virus, and the number of infected are in scattered form. During the lockdown phase, the infection is still increasing its rate, but as the unlock 1.0 started, a massive gain in the number of infected can be observed from the Fig. 5. The 7-days moving average curves signify the growing pattern in the data set for the advancement of time. This increasing trend of the curves leads us to approximate the data curves by some known mathematical functions. Following Sun et al. [18],

we assume an exponential growth curve for the cumulative number of confirmed cases in India for each of the groups as mentioned earlier. We consider the cumulative number of confirmed cases in India from March 01, 2020 to June 30, 2020 with the form $y(t) = a \exp(bx + c) + d$, where a , b , c and d are positive constants, to be estimated. The resulting curves are shown in Fig. 6.

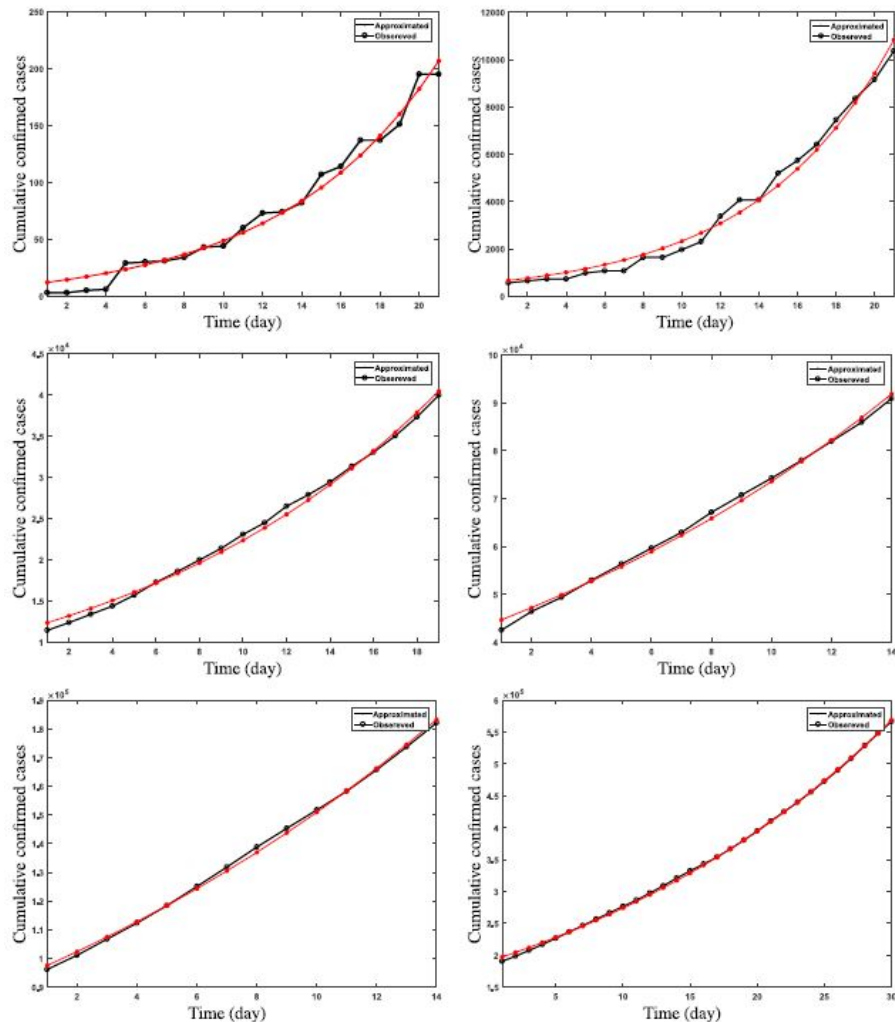


Figure 6.
Observed data curve is approximated by exponential growth curve

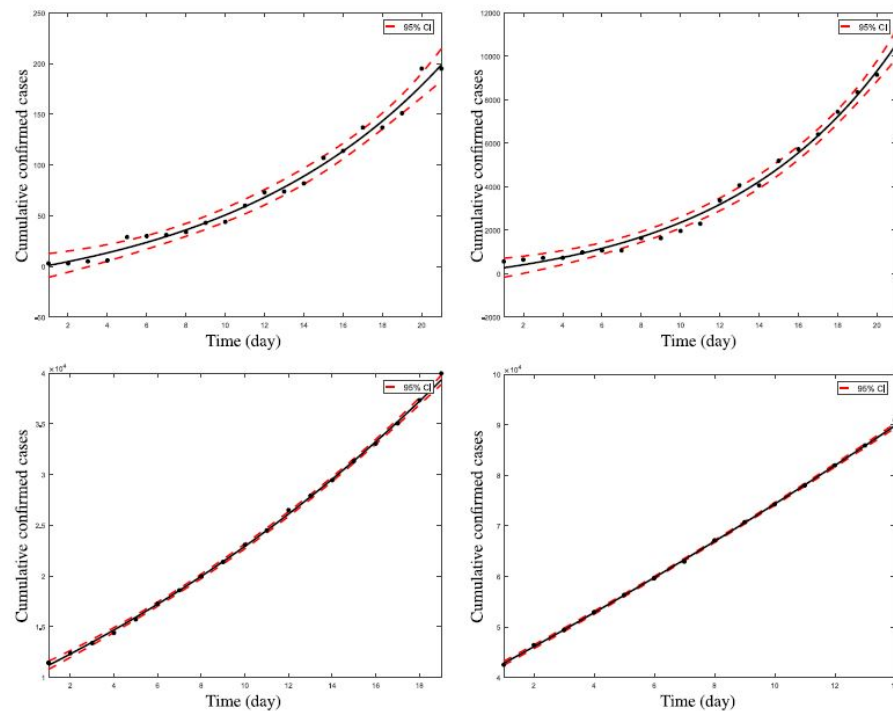


Figure 7.

95% confidence interval for the observed data for the before lockdown stage (March 1–21), the first, the second and the third phases of lockdown (March 25–April 14, April 15–May 3, May 4–17, respectively).

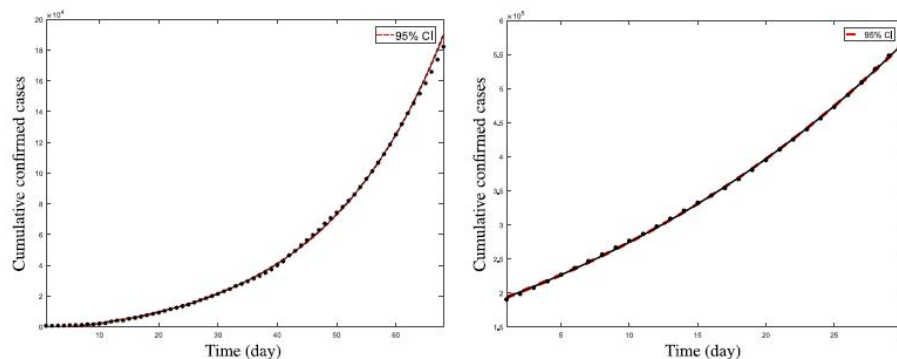


Figure 8.

95% Confidence interval for the observed data for the overall lockdown phases and the phase of unlock 1 (June 1–30).

To estimate the parameters a , b , c and d , the least-square approximation is used, and 95% confidence interval has been shown in Figs. 7 and 8. The estimated values of the parameter has also been shown in Table 5. In statistics, a confidence interval measures the probability that a parameter will fall between a pair of values around the mean for a certain proportion of times. The exact values of the corresponding confidence interval is given as (0.6844, 0.1658, 2.4751, 0.1136).

Table 5.

Confidence interval for the parameters involved in the exponential growth curve.

Parameters	95% confidence interval	Parameters	95% confidence interval
a	(0.5094, 0.8593)	c	(2.3554, 2.5948)
b	(0.1530, 0.1785)	d	(-19.7617, 19.9890)

5.2 Effect of quarantine and isolation

Simulation results for the number of confirmed COVID-19 cases with various lockdown strategies dates (March 25, April 15, May 04 and May 18) in India are shown in Fig. 9. We will discuss about the effect of ρ , σ , n_1 and n_2 on the epidemic trend and the final scale. The implementation of the lockdown measures in India indicates that the lower rate of the quarantine ρ and isolation σ , the peak of the newly infected people in the city will increase and higher the final scale. In Fig. 9, the highest dark blue curve corresponds to the value of the number of infected for $\rho = 0.01$, and as the value of ρ get increased, the peak of the curve decreases as we can see from the red, yellow, violet and other curves. Likewise, for the isolation rate σ become larger, the peak of the curve flattens as indicated by the blue, green, violet curves, respectively. This shows an obvious influence of quarantining and isolating of the infected individuals. As much as we can trace the infected individuals and keep them distant from the susceptible population, it would be more effective to control and take step towards the eradication of the disease.

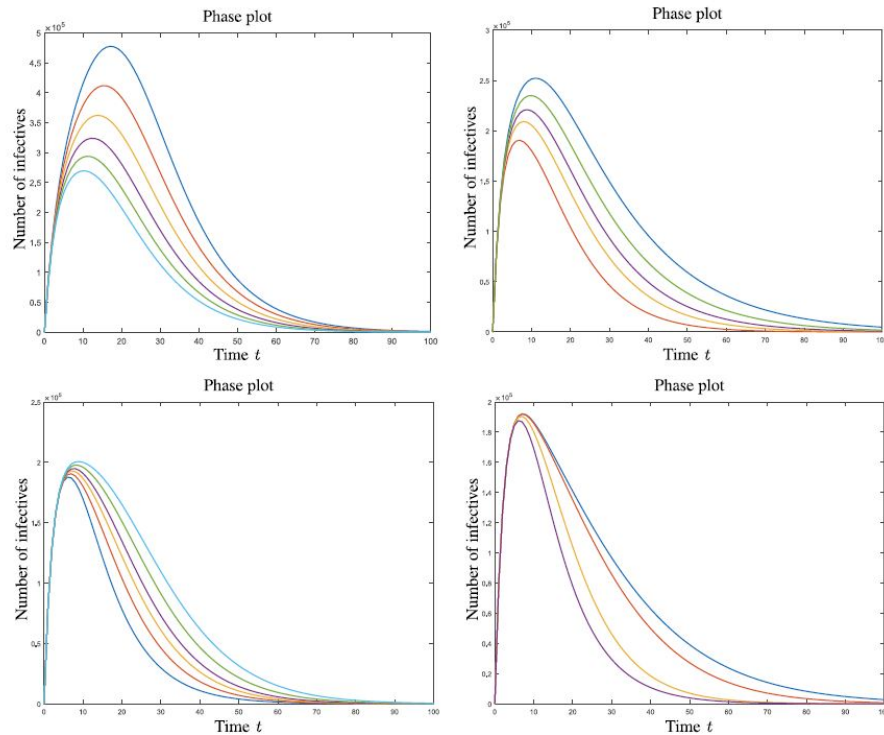


Figure 9.

Simulation results for change of the number of infective with respect to: (a) the quarantine rate ρ , (b) the isolation rate σ , (c) the rate of return to susceptible class η_1 and (d) the rate of progression to infectiousness η_2 .

On the other hand, the infection data curve shows that as the value of n_1 rises, the peak and the scattering of the infected curve falls downward. Although, the increase in n_2 leads to opposite nature of the curve. The value of n_2 is highest for the violet curve, and for that, it can be seen that the scattering of the curve is smaller than the rest curves. Thus, in conclusion, one can say that apart from proper medical treatment, the consistent effort of quarantine and isolation can lead to an effective control measure for COVID-19. Since no proper vaccination is still available for all and the disease is highly contagious, the quarantining and isolation are the most effective strategies now a days in India. The lockdown strategy strength can be enhanced by proper way of tracing the individuals, who have get in contact with the infected, testing them and finally categorize them into the susceptible and infected class.

6 Conclusions and discussions

In this paper, an epidemic $SEQ_1 IQ_2 R$ model is designed to describe the transmission dynamics of COVID-19 in India. The positivity and boundedness of the proposed model is established. Explicit Euler method with the time step size $\Delta t = 0.01$ is used to integrate system (1) on Matlab R2016b platform. The control reproduction number R_c has been calculated, and its nature with respect to quarantine rate is simulated for different values of transmission coefficient β . Then an optimal period for

quarantine and isolation has been calculated (c.f. Fig. 3). The sensitivity analysis of R_c with respect to the control parameters ρ and σ has been performed. Also, to identify the influence of the parameters, we used the PRCC method. Next, on the basis of the data given in [25], for the initial prelockdown phase (March 01, 2020 onwards) up to the first unlock phase (June 30, 2020), we estimated the parameters, which are used to trace data curve. Using the least squares approximation for the parameters, 95% confidence interval had been established. The effect of control strategies such as the quarantine rate, isolation rate, rate of coming back to the susceptible class and rate of progression to infectiousness are shown by the simulated figures.

From Fig. 5 we can see a gradual increase in the number of daily infected cases. Initially, in the prelockdown stage, the rate of increase of the number of daily cases are gradually increasing. When the lockdown started, the 7-days moving average curve shows that the number of cases per day in India rapidly increased, but due to the governmental policies like, the process of quarantine and isolation restricted this increment, and the outbreak was under control. As the unlock phase started, the prevalence was out of control. The nature of the data curve seems to be always increasing, and thus, an exponential growth curve is used to approximate the observed data as shown in Fig. 6. Further, Figs. 7 and 8 explain the 95% confidence interval for the corresponding approximated exponential curves. Incidentally, the generalized form of exponential growth curve approximates the cumulative data curve appropriately, which indicates that the growth rate of COVID-19 is expeditious in nature, but in the presence of the control measures and strict lockdown, the disease propagation can be managed. The controlled reproductive number R_c of COVID-19 has been initially estimated by the WHO in the range between 1 and 2.5 as declared in the statement regarding the outbreak of SARS-CoV-2 dated 23rd January 2020 mentioned in Viceconte and Petrosillo [22]. Several studies are still now trying to develop the proper measure of control and to estimate the reproduction number of the current pandemic. Other important factors are that no proper treatment facilities are available for all such as required number of hospital beds, enough supply of oxygen and shortage of the medicine like *remdesivir*. Also, the vaccination procedure is restricted from some particular age group of people, and it is not of absolute efficacy to stay distant to COVID-19, but only to stay at home and maintaining physical distances in the society. Although, tracing out the infected individuals and their surroundings, testing sufficient number of the individuals and treating them in a proper way such as by keeping them isolated, one can take steps towards the progress in the way to get away from this current pandemic situation.

In our model, we have taken both the strategies of quarantine and isolation and showed the relationship of the quarantine and isolation rate with the controlled reproduction number R_c . Further, models on COVID-19 can be constructed either by incorporating time-delay as a latent period to have the symptoms or by taking reaction–diffusion sys-

tem for modeling the spread dynamics. One may update the proposed model system in the reaction–diffusion platform in order to explore the temporal as well as the spatial dynamics that will strengthen our study in a new direction in future.

References

- 1 S. Çakan, Dynamic analysis of a mathematical model with health care capacity for COVID-19 pandemic, *Chaos Solitons Fractals*, **139**:110033, 2020, <https://doi.org/10.1016/j.chaos.2020.110033>.
- 2 I. Cooper, A. Mondal, C.G. Antonopoulos, A SIR model assumption for the spread of COVID-19 in different communities, *Chaos Solitons Fractals*, **139**:110057, 2020, <https://doi.org/10.1016/j.chaos.2020.110057>.
- 3 P. Van den Driessche, Reproduction numbers of infectious disease models, *Infectious Disease Modelling*, **3**:288–303, 2017, <https://doi.org/10.1016/j.idm.2017.06.002>.
- 4 P. Van den Driessche, J. Watmough, Reproduction numbers and sub-threshold endemic equilibria for compartmental models of disease transmission, *Math. Biosci.*, **180**(1–2):29–48, 2002, [https://doi.org/10.1016/S0025-5564\(02\)00108-6](https://doi.org/10.1016/S0025-5564(02)00108-6).
- 5 P. Van den Driessche, J. Watmough, Further notes on the basic reproduction number, in *Mathematical Epidemiology*, Springer, Berlin, Heidelberg, 2008, pp. 159–178, <https://doi.org/10.1007/978-3-540-78911-6>.
- 6 O. Diekmann, J.A.P. Heesterbeek, *Mathematical Epidemiology of Infectious Diseases: Model Building, Analysis and Interpretation*, Wiley Ser. Math. Comput. Biol., Vol. 5, John Wiley & Sons, Chichester, 2000.
- 7 Z. Feng, H.R. Thieme, Recurrent outbreaks of childhood diseases revisited: The impact of isolation, *Math. Biosci.*, **128**(1–2):93–130, 1995, [https://doi.org/10.1016/0025-5564\(94\)00069-C](https://doi.org/10.1016/0025-5564(94)00069-C).
- 8 D. Gilbert, How does coronavirus compare to flu, sars, and other diseases?, <https://www.telegraph.co.uk/news/0/coronavirus-vs-sars-mers-flu-how-deaths-compare-covid-19/>.
- 9 J.M. Heffernan, R.J. Smith, L.M. Wahl, Perspectives on the basic reproductive ratio, *J. R. Soc. Interface*, **4**:281–293, 2005, <https://doi.org/10.1098/rsif.2005.0042>.
- 10 S. Marino, I.B. Hogue, C.J. Ray, D.E. Kirschner, A methodology for performing global uncertainty and sensitivity analysis in systems biology, *J. Theor. Biol.*, **254**(1):178–196, 2008, <https://doi.org/10.1016/j.jtbi.2008.04.011>.
- 11 M. Martcheva, *An Introduction to Mathematical Epidemiology*, Texts Appl. Math., Vol. 61, Springer, Boston, MA, 2015, <https://doi.org/10.1007/978-1-4899-7612-3>.
- 12 G. Rohith, K.B. Devika, Dynamics and control of COVID-19 pandemic with nonlinear incidence rates, *Nonlinear Dyn.*, **101**(3):2013–2026, 2020, <https://doi.org/10.1007/s11071-020-05774-5>.
- 13 P. Roy, R.K. Upadhyay, J. Caur, Modeling Zika transmission dynamics: Prevention and control, *J. Biol. Syst.*, **28**(3):719–749, 2020, <https://doi.org/10.1142/S021833902050014X>.

- 14 T. Sardar, S.S. Nadim, S. Rana, J. Chattopadhyay, Assessment of lockdown effect in some states and overall India: A predictive mathematical study on COVID-19 outbreak, *Chaos Solitons Fractals*, **139**:110078, 2020, <https://doi.org/10.1016/j.chaos.2020.110078>.
- 15 R. Scheult, Coronavirus outbreak – transmission & updates explained, January 2020, <https://www.youtube.com/watch?v=9vMXSkKLg2I>.
- 16 M.A. Shereen, S. Khan, A. Kazmi, N. Bashir, R. Siddique, Covid-19 infection: Origin, transmission, and characteristics of human coronaviruses, *J. Adv. Res.*, **24**:91–98, 2020, <https://doi.org/10.1016/j.jare.2020.03.005>.
- 17 N.I. Stilianakis, Y. Drossinos, Dynamics of infectious disease transmission by inhalable respiratory droplets, *J. R. Soc. Interface*, **7**(50):1355–1366, 2010, <https://doi.org/10.1098/rsif.2010.0026>.
- 18 G.Q. Sun, S.-F. Wang, M.-T. Li, L. Li, J. Zhang, W. Zhang, Z. Jin, G.-L. Feng, Transmission dynamics of COVID-19 in Wuhan, China: Effects of lockdown and medical resources, *Nonlinear Dyn.*, **101**(3):1981–1993, 2020, <https://doi.org/10.1007/s11071-020-05770-9>.
- 19 R. Taylor, Interpretation of the correlation coefficient: A basic review, *J. Diagn. Med. Sonogr.*, **1**(1):35–39, 1990, <https://doi.org/10.1177/875647939000600106>.
- 20 H. Tian, Y. Liu, Y. Li, C.-H. Wu, X. Chen, M.U.G. Kraemer, B. Li, J. Cai, B. Xu, Q. Yang, B. Wang, P. Yang, Y. Cui, Y. Song, P. Zheng, Q. Wang, O.N. Bjornstad, R. Yang, B.T. Grenfell, O.G. Pybus, C. Dye, An investigation of transmission control measures during the first 50 days of the COVID-19 epidemic in China, *Science*, **368**(6491):638–642, 2020, <https://doi.org/10.1126/science.abb6105>.
- 21 R.K. Upadhyay, S. Chatterjee, S. Saha, R.K. Azad, Age-group-targeted testing for COVID-19 as a new prevention strategy, *Nonlinear Dyn.*, **101**(3):1921–1932, 2020, <https://doi.org/10.1007/s11071-020-05879-x>.
- 22 G. Viceconte, N. Petrosillo, COVID-19 R0: Magic number or conundrum?, *Infectious Disease Reports*, 2020, <https://doi.org/10.4081/idr.2020.8516>.
- 23 R. Woelfel, V.M. Corman, W. Guggemos, M. Seilmaier, S. Zange, M.A. Mueller, D. Niemeyer, P. Vollmar, C. Rothe, M. Hoelscher, T. Bleicker, Clinical presentation and virological assessment of hospitalized cases of coronavirus disease 2019 in a travel-associated transmission cluster, *MedRxiv*, 2020, <https://doi.org/10.1101/2020.03.05.20030502>.
- 24 J. Wu, R. Dhingra, M. Gambhir, J.V. Remais, Sensitivity analysis of infectious disease models: Methods, advances and their application, *J. R. Soc. Interface*, **10**(86):20121018, 2013, <https://doi.org/10.1098/rsif.2012.1018>.
- 25 Situation Reports 2019, <https://www.who.int/emergencies/diseases/novel-coronavirus-2019/situation-reports>.
- 26 The Times of India, Ranchi Edition, VIII(10):1–18, <https://timesofindia.indiatimes.com/city/ranchi>.